



HAL
open science

Performance Evaluation of Controller Design Based on Accurate Model of Non-Inverting Buck Boost Converter Fed by Photovoltaic Module

Yaosuo Li, Kai Liu, Hui Wang, Min Gu

► **To cite this version:**

Yaosuo Li, Kai Liu, Hui Wang, Min Gu. Performance Evaluation of Controller Design Based on Accurate Model of Non-Inverting Buck Boost Converter Fed by Photovoltaic Module. American Scientific Research Journal for Engineering, Technology, and Sciences (ASRJETS), 2017, 30 (1). hal-01503898

HAL Id: hal-01503898

<https://hal.science/hal-01503898v1>

Submitted on 7 Apr 2017

HAL is a multi-disciplinary open access archive for the deposit and dissemination of scientific research documents, whether they are published or not. The documents may come from teaching and research institutions in France or abroad, or from public or private research centers.

L'archive ouverte pluridisciplinaire **HAL**, est destinée au dépôt et à la diffusion de documents scientifiques de niveau recherche, publiés ou non, émanant des établissements d'enseignement et de recherche français ou étrangers, des laboratoires publics ou privés.

Performance Evaluation of Controller Design Based on Accurate Model of Non-Inverting Buck Boost Converter Fed by Photovoltaic Module

YAOSUO Li^a, Kai Liu^b, Hui Wang^c, Min Gu^{d*}

^{a,b,c,d}*Department of Electrical Engineering Guangdong University of Foreign Studies Guangzhou, China*

^d*Email: min.gu1980@gmail.com*

Abstract

The design of controller based on simplified models can lead to difference between expected and practical results or even instability of the converter. Therefore, obtaining an accurate model is of great importance. In this paper, firstly, the accurate model of non-inverting buck boost converter by considering all parasitic components is obtained. Then, two PI and Type 3 controllers are designed based on accurate model. Afterwards, the performance of these controllers is compared with controllers designed based on a simplified model. All tests are carried out on a prototype of a non-inverting buck boost connected a photovoltaic module. The obtained results show the controllers designed based on accurate model have superior performance in comparison with controllers designed based on simplified model. In addition, the bode diagram obtained based on analog method in PSIM software and the one obtained based on transfer function of accurate model confirm the accuracy of the derived model.

Keywords: Non-inverting buck boost; small signal model; photovoltaic systems; state space model.

1. Introduction

Extensive use of dc-dc power converters in many of industrial applications from one side, and considerable attention to their performance from another side, makes them to an attractive topic in power electronics [1-11]. In many applications of dc-dc power converters, usually a wide range of operation for input and output voltages is required. For instance, the output voltage of a photovoltaic module can be variable in according to temperature or sun angle, hence, if a certain output voltage is required, a converter that is able to increase or decrease of its input voltage is necessary [12-15]. Due to the ability of non-inverting buck boost converters to work in buck, boost and buck-boost modes, this goal can be fulfilled. Figure 1 depicts a non-inverting buck boost fed by a photovoltaic module. In addition, simple structure, low stress on switches and positive polarity of output voltage make this converter a suitable choice for this application [16,17-26].

* Corresponding author.

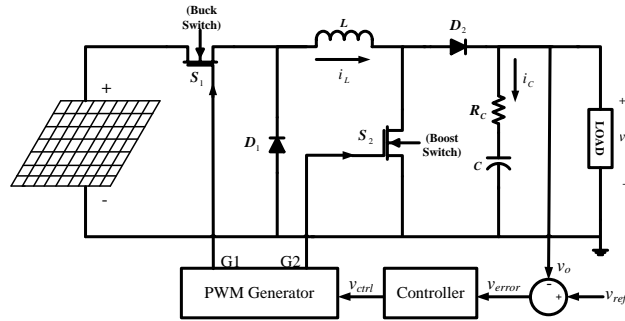


Figure 1: Non-inverting buck boost connected to a PV and in presence of control system

To study the converter characteristic, the first step is to obtain the system model for each of its operation modes. A conventional solution to obtain the dynamic model of the system is state space averaging model [16,27,28]. In [29], linearized state space models for buck, boost and non-inverting buck boost converters have been presented. Although huge efforts have been conducted to apply non-linear methods to control non-linear converters in recent years [30], owing to simplicity and generality of control method based on linearized state space models could maintain their popularity. In [31], a large signal transient model for dc-dc converter has been proposed. In addition, average state space model of conventional buck-boost converter in presence of all parasitic components has been presented in [32].

Under boost mode operation, the converter has non-minimum phase performance and as a result, in absence of a closed loop controller, the system is unstable. Therefore, the design of a closed loop controller is of great importance.

In the previously reported model for non-inverting buck-boost converters, only the effect of equivalent series resistance (ESR) of capacitor has been considered. In this paper, the complete model of the converter, with considering all parasitic components of the circuit is proposed and a general transfer function for buck and boost mode is derived. To show the accuracy of the proposed model, a 45 w PV module is used as input voltage source of the converter. The performance of the PI and Type3 controllers designed based on the accurate model of the system is compared with the same controllers' performance just designed based on simplified model of the converter. The obtained results of the performance of the converter in presence of different controllers and under a step change in the output power of the PV modules are provided.

2. Linearized Average State Space Modle

A non-inverting buck boost converter is a combination of buck and boost converters. It consists of two switches and has only one inductor and one capacitor. To achieve a desired performance, having an accurate model of the converter is necessary. To obtain accurate state space model of non-inverting buck boost converter, firstly, the switching strategy for two switches should be determined. In this converter, if both switches are controller with

the same duty cycle and constant switching frequency, the similar performance as the buck-boost converter is achieved. If the switches work with constant switching frequency but with different duty cycles, the operation will be different. Consider S_2 is continuously off during a control period, while S_1 turns on and off. Under this condition, buck operation will be yielded. When S_1 is always on and S_2 is switching, the converter works on boost mode. Due to high losses of working in buck-boost mode in comparison with buck and boost modes, this operation mode is avoided. Table 1 summarizes the switching state when the converter works on each of its operation mode. Now, after determination of the operation states of the converter, small signal transfer function of the converter can be derived as the following.

In buck operation and only by considering equivalent resistance of the capacitor (R_c), small signal transfer function of control input (\hat{d}) and disturbance source (\hat{v}_{in}) to output voltage (\hat{v}_o) can be obtained as follows [29].

$$\hat{v}_o = \frac{V_{in}(1+R_cCs)}{s^2 + \frac{s}{RC} + \frac{1}{LC}} \hat{d} + \frac{D_1(1+R_cCs)}{s^2 + \frac{s}{RC} + \frac{1}{LC}} \hat{v}_{in} \quad (1)$$

To work in boost mode, small signal transfer function is as follows

$$\hat{v}_o = \frac{\frac{I_L}{C} \left(\frac{V_{in}}{LI_L} - s \right) (1+R_cCs)}{s^2 + \frac{s}{RC} + \frac{(1-D_2)^2}{LC}} \hat{d} + \frac{(1-D_2)(1+R_cCs)}{s^2 + \frac{s}{RC} + \frac{(1-D_2)^2}{LC}} \hat{v}_{in} \quad (2)$$

In the above equations, R , C and L are resistor, capacitor and inductor values in the converter. D_1 and D_2 are duty cycles of S_1 and S_2 in the steady states. In addition, I_L denotes the inductor current and V_{in} shows input voltage in the steady state. The quantities with “^” are small variation around steady state operating point.

Table 1: Switching Table

<i>Operation Mode</i>	S_1	S_2
Buck	Switching	Off
Boost	On	Switching
Buck-Boost	Switching	Switching

Table 2: Simulation and Experimental Parameters

V_{in}	14- 18V
V_o	16 V
f_s	50 kHz

L 50 μH
 R_o 30 Ω
 C 1.8 mF

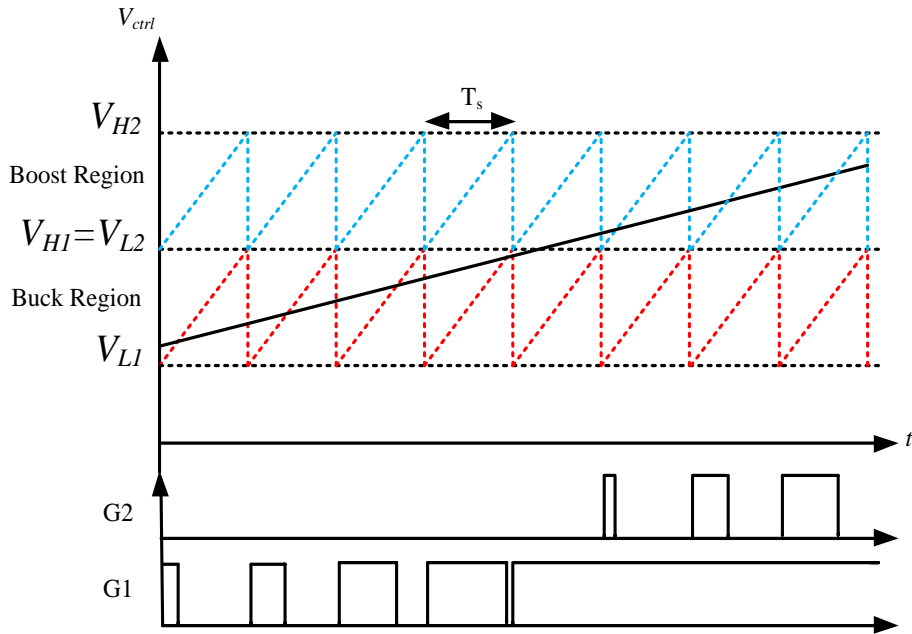


Figure 2: PWM generations of switches in non-inverting buck boost

3. Converter Transfer Function Analysis

4. Frequency Domain Analysis

A conventional method to analysis the stability of a system is the analysis the frequency response of the system using its bode diagram [33].

Figure 4 shows the bode diagram of control signal (duty cycle) to output voltage for buck and boost operation mode when parameters presented in Table 2 is used. As it can be seen from Figure 4, although stability margins in the buck mode is appropriate, the phase and gain margin in the boost mode is negative and therefore system is unstable. Therefore, a controller should be designed based on the worst case, i.e. boost mode operation. As it can be seen from (2), a right half plan zero exists in the transfer function and its value depends on inductance value, inductance current and input voltage.

The right half plan zero (RHPZ) in the transfer function of a system adds negative phase to the system and consequently, causes some limitation in bandwidth selection in process of design a linear controller.

The physical effect of RHPZ has been shown in [34]. It has been demonstrated that RHPZ causes underdamp and therefore oscillation in the output voltage of the system. According to Figure 1, firstly, the output voltage is measured and then, it is compared with the reference and its error is fed to the controller. Figure 2 depicts the switches gate signal generation in according to output signal of the controller. As it can be observed, the switches' state is determined by comparing the triangle carrier waveform with output of the controller. In this

figure, V_{H1} and V_{L1} are maximum and minimum voltages of carrier waveform in buck mode, respectively, and V_{H2} and V_{L2} are similar quantities in the boost mode. $G1$ and $G2$ are gate signals of S_1 and S_2 , respectively.

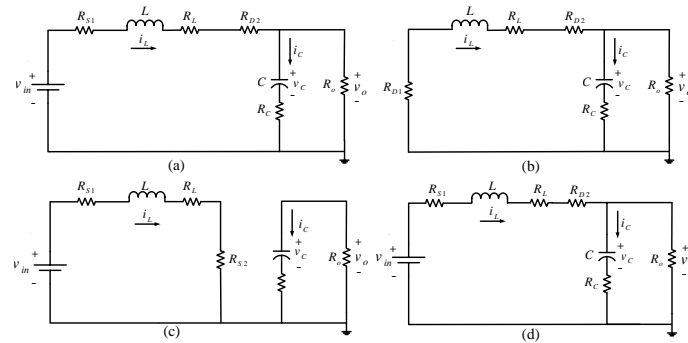


Figure 3: Equivalent circuit of the non-inverting buck boost converter with parasitic element (a) buck mode when switch is on (b) buck mode when switch is off (c) boost mode when switch is on (d) boost mode when switch is off

5. Controller Design and Selection

The most serious problems of open loop operation of non-inverting buck-boost converter are: (1) negative phase and gain margins in boost mode, which leads to instability (2) system is zero type (given the zero slope of gain diagram in low frequencies) that leads to steady state error. Hence, the employed controller in the closed loop system should be able to deal with these issues. PI and Type3 controllers are two conventional linear controller to control of dc-dc converters [35,37-40]. The following expressions show transfer functions of PI and Type3 controllers

$$C1(s) = K_p + \frac{K_i}{s} \quad (3)$$

$$C2(s) = \frac{K_3 s^2 + K_2 s + K_1}{s(K_6 s^2 + K_5 s + K_4)} \quad (4)$$

The zero pole of these controllers provide high gain in low order frequencies and this issue can eliminate the steady state error and improve the phase margin.

6. Complete Model of Non-Inverting Buck Boost

a. Complete Transfer Function

The complete model of the converter is developed based on the equivalent circuit of the converter in different operation modes. Figure 3 shows the equivalent circuits of the converter. In this figure, R_L is equivalent resistor of the inductor, R_D and R_S denote turn on resistor of the diode and switches, respectively.

In according to the importance of controller design and stability analysis of the converter in the boost mode, only the complete model of the converter in the boost mode is discussed in this section. It is noteworthy that in the buck mode similar results can be obtained. In the boost mode, according to Figure 3 (c), the state space

equations can be expressed as

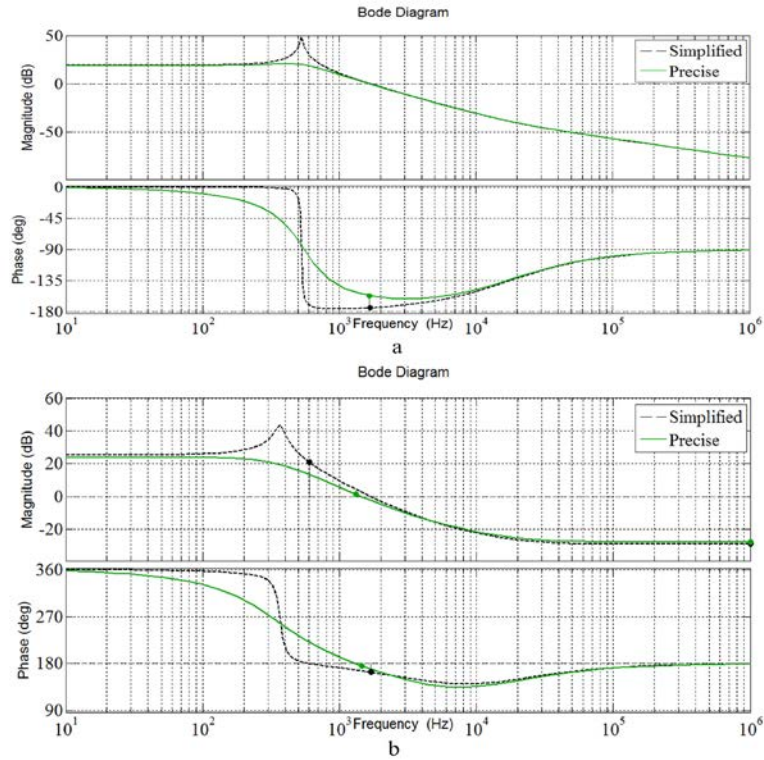


Figure 4: Diagram bode of simplified and accurate models (a) buck mode (b) boost mode

$$\begin{cases} \dot{x} = A_1x + B_1u \\ y = C_1x + D_1u \end{cases}, x = \begin{bmatrix} i_L \\ v_C \end{bmatrix}, u = v_{in}, y = v_o \quad (5)$$

$$A_1 = \begin{bmatrix} \frac{-(2R_s + R_L)}{L} & 0 \\ 0 & \frac{-1}{\Delta} \end{bmatrix}, B_1 = \begin{bmatrix} \frac{1}{L} & 0 \\ 0 & \frac{-R_o}{\Delta} \end{bmatrix}, \quad (6)$$

$$C_1 = \begin{bmatrix} 0 & 1 - \frac{CR_C}{\Delta} \end{bmatrix}, D_1 = \begin{bmatrix} 0 & \frac{-CR_C R_o}{\Delta} \end{bmatrix}$$

in which, $\Delta = R_o C + R_C C$ and the following assumptions are made to simplify the calculation

$$R_{S1} = R_{S2} = R_S, \quad R_{D1} = R_{D2} = R_D \quad (7).$$

When switch is on (see Figure 3 (d)), the state space equation is as follows

$$\begin{cases} \dot{x} = A_2x + B_2u \\ y = C_2x + D_2u \end{cases} \quad (8)$$

Eventually, to obtain the average model in the boost mode, the equations corresponding to on-time and off-time of switch are combined as follows

$$\begin{aligned}
 A_2 &= \begin{bmatrix} -\left(\frac{R_s + R_L + R_D}{L} + \frac{CR_C R_o}{\Delta L}\right) & \left(\frac{CR_C}{L\Delta} - \frac{1}{L}\right) \\ \frac{R_o}{\Delta} & \frac{-1}{\Delta} \end{bmatrix}, \\
 B_2 &= \begin{bmatrix} \frac{1}{L} & \frac{CR_C R_o}{L\Delta} \\ 0 & \frac{-R_o}{\Delta} \end{bmatrix}, \\
 C_2 &= \begin{bmatrix} R_o - \frac{CR_o^2}{\Delta} & \frac{CR_o}{\Delta} \end{bmatrix}, D_2 = \begin{bmatrix} 0 & \frac{CR_o^2}{\Delta} - R_o \end{bmatrix}
 \end{aligned} \tag{9}$$

$$\begin{cases} \dot{x}_p = A_p x + B_p u \\ y_p = C_p x + D_p u \end{cases} \tag{10}$$

$$\begin{cases} A_p = A_1 d + A_2 (1-d) \\ B_p = B_1 d + B_2 (1-d) \\ C_p = C_1 d + C_2 (1-d) \\ D_p = D_1 d + D_2 (1-d) \end{cases} \tag{11}$$

To obtain the state variable X around operating point, the following equations is used

$$\dot{x} = A_p x + B_p u = 0 \Rightarrow X = -A_p^{-1} B_p U \tag{12}$$

To derive the linear transfer function of the system in the boost mode, the above nonlinear equations should be linearized around operating point. To this end, state variable and system inputs are considered as a constant term (DC) and a term showing the small variation around operating point. So,

$$\begin{cases} x(t) = X + \hat{x} \\ d(t) = D + \hat{d} \\ u(t) = U + \hat{u} \\ v_o(t) = V_o + \hat{v}_o \end{cases} \tag{13}$$

By substituting (13) into (10),

$$\begin{cases} \dot{X} + \hat{\dot{x}} = A_p \hat{x} + B_p \hat{u} + [A_{12} X + B_{12} U] \hat{d} + \dot{X} \\ \dot{V}_o + \hat{\dot{v}}_o = C_p \hat{x} + D_p \hat{u} + [C_{12} X + D_{12} U] \hat{d} + \dot{V}_o \end{cases} \tag{14}$$

where,

$$\begin{cases} A_{12} = A_1 - A_2 \\ B_{12} = B_1 - B_2 \\ C_{12} = C_1 - C_2 \\ D_{12} = D_1 - D_2 \end{cases} \quad (15)$$

As a result, the output voltage variations can be expressed as

$$\hat{v}_o = [C_p(SI - A_p)^{-1}(A_{12}X + B_{12}U) + (C_{12}X + D_{12}U)] \hat{d} + (C_p(SI - A_p)^{-1}B_p + D_p) \hat{u} \quad (16)$$

Since \hat{d} is the only control signal for the converter, the transfer function of output to control signal for the boost mode is as

$$G(s) = \frac{\hat{v}_o}{\hat{d}} = \frac{a_3s^2 + a_2s + a_1}{b_3s^2 + b_2s + b_1} \quad (17)$$

in which,

$$\begin{aligned} a_3 &= -V_{in}CLR_C D', a_2 = -V_{in}L \\ a_1 &= V_{in}(R_o D'^2 - R_L), b_3 = CL(R_o D'^2 + R_D + R_L) \\ b_2 &= CR_C R_o (-3DD' + 1) + \\ &CR_o D'(R_D D'^2 + R_S + R_L D') + LD'^2 \\ b_1 &= 2R_D (-3DD' + 1) - 4R_L D + 2R_L + R_o D'^4 \end{aligned} \quad (18)$$

Also, $D' = 1 - D$ and

$$D = \frac{(V_o - V_{in} + R_S + R_D + R_L)I_L}{(R_S I_L - V_o - R_D I_L)} \quad (19)$$

In the above equations, I_L can be replaced by (12). To simplify the final transfer function, with an acceptable approximation, the terms with low order have been neglected.

The same procedure can be repeated for the buck mode. The transfer function of buck mode is as follows

$$\begin{aligned} G(s) &= \frac{\hat{v}_o}{\hat{d}} = \frac{a_3s^2 + a_2s + a_1}{b_3s^2 + b_2s + b_1} \\ a_3 &= -V_{in}CLR_C D', a_2 = -V_{in}L \\ a_1 &= V_{in}(R_o D'^2 - R_L), b_3 = CL(R_o D'^2 + R_D + R_L) \\ b_2 &= CR_C R_o (-3DD' + 1) + \\ &CR_o D'(R_D D'^2 + R_S + R_L D') + LD'^2 \\ b_1 &= 2R_D (-3DD' + 1) - 4R_L D + 2R_L + R_o D'^4 \end{aligned} \quad (20)$$

$$D = \frac{V_o + (2R_D + R_L)I_L}{V_{in} + (R_D - R_S)I_L} \quad (21)$$

In Figure 4, the bode diagram of simple and complete model are compared.

Considering the stability margins, one can see that the stability and dynamic of the system by considering the parasitic components are significantly ameliorated.

Table 3 module parameters under standard test condition (STC)

V_{oc}	21.9 V
V_{MPP}	17.6 V
I_{sc}	2.7 A
I_{MPP}	2.56 A
P_{MPP}	45 W

Table 4: Parasitic elements of the converter

R_L	100 m Ω
R_C	5 m Ω
$R_{S1}=R_{S2}$	7.8 m Ω
$R_{D1}=R_{D2}$	80 m Ω

Table 5 Parameters of PI controller designed based on simplified and complete model

<i>Controller Parameter</i>	<i>Simplified Model</i>	<i>Complete Model</i>
K_p	0.00054	0.02026
K_i	3.434	38.19

7. Simulation and Experimental Results

To evaluate the performance of the control system and to provide a fair comparison between designed controllers, a prototype of a non-inverting buck boost converter fed by a PV module is used (see Figure 5). The goal of tests is to assess the ability of the control system to maintain the output voltage of the converter under change in the PV condition. Table III summarizes the parameters of PV module under standard test condition (STC) and table 4 shows the parasitic parameters of the converter.

In the designed converter, instead of each diode two parallel diode is used to improve the converter power

rating. So, the resistor of these two diode equivalently is considered as the on-time resistor of the diode. In addition, R_L value includes the sum of resistor of PCB routes and also, it is by considering the increase of inductor resistor because of skin effect in switching frequency of 50 kHz. In Figure 6, a comparison between the bode diagram obtained by simulation of the converter in PSIM software and block diagram based on the complete transfer function of the system is carried out. As it can be observed, the similarity of two bode diagrams shows the accuracy of the developed model. To design PI and Type3 controllers the classic design method in frequency domain is employed. The controller parameters designed based on two models are in Table V.

To provide a change in the input voltage of the converter, the sun radiation artificially changes. Since the load power is constant, by changing the sun radiation, the input voltage will disturb. Therefore, in the implemented test, the converter firstly works in the buck mode, then, after change in the sun radiation and power reduction it goes to boost mode and continue to work in this mode. It worth noting that the PV voltage during these variations reduces from 18 Volt to 15 Volt, while the control system keeps the output voltage of the controller at 16 Volt. As it can be shown in Figure 7, the PI controller designed based on the complete model has significantly superior dynamic performance in comparison with PI designed based on simplified model. Due to freedom degree of Type3 controller in comparison with PI controller, the cut-off frequency of the controller can be chosen at higher frequency and hence, it has faster dynamic than PI. Figure 7 (c) and (d) compares the performance of the Type3 controllers designed based on two models. As it can be expected, the Type3 based on complete model has faster dynamic.

Table 6: Parameters of Type3 controller designed based on simplified and complete model

Controller Parameter	Simplified Model	Complete Model
K_1	41.64	50.3
K_2	0.07258	0.07244
K_3	3.16e-5	2.6e-5
K_4	1	1
K_5	5.8e-5	1.43e-4
K_6	8.4e-10	5.1e-9

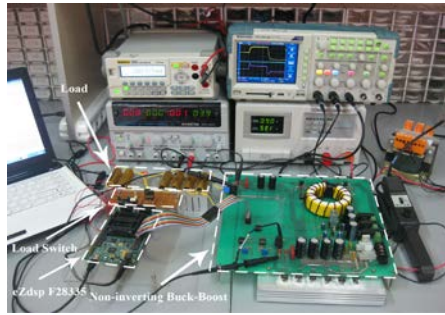


Figure 5: A scheme of non-inverting buck boost converter

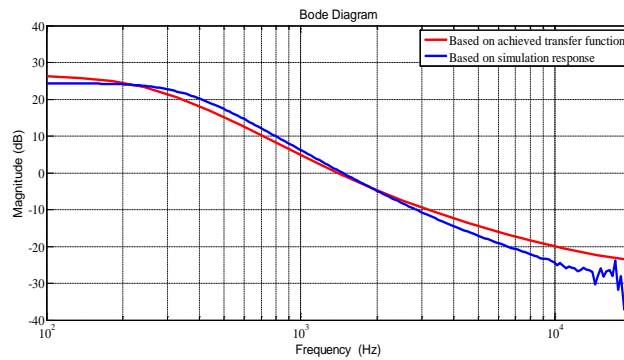


Figure 6: Diagram bode based on PSIM simulation and based on accurate transfer function of the converter

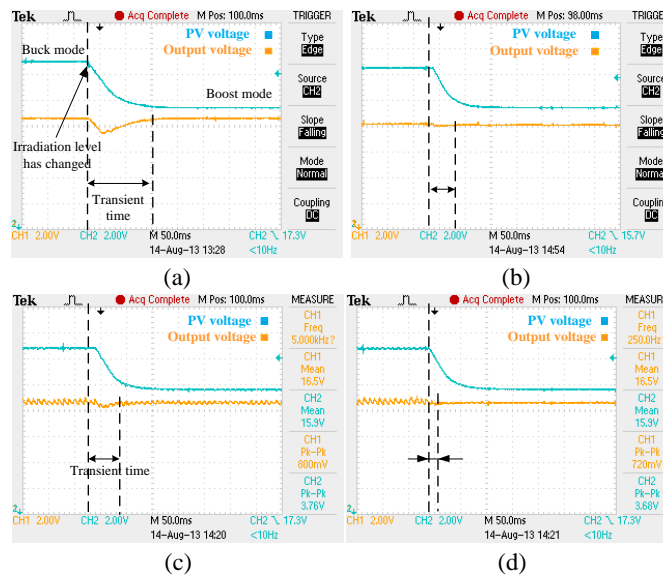


Figure7: Output voltage and input voltage of the converter when a change occurs in the PV for (a) PI based on simplified model (b) PI based on complete model (c) Type3 based on simplified model (d) Type3 based on complete model

8. Coclusion

In this paper, the complete model of the non-inverting buck-boost converter in presence of all parasitic

components has been proposed. After obtaining the complete model of the converter, the dynamic analysis between the transfer function of the simplified model and complete model has been carried out. Then, two PI and Type3 controllers are designed based on frequency response of the system. The experimental results for the controllers designed based on complete mode, show the better performance of them to regulate the output voltage of a PV module.

References

- [1] H. Jafarian, B. Parkhideh, and S. Bhowmik "Robustness Evaluation of Grid-tied AC-stacked PV Inverter System Considering Manufacturing Inaccuracies" 42nd Annual IEEE Conference of Industrial Electronics Society (IECON), Florence, 2016, (In press)
- [2] M. Dabbaghjamanesh, A. Moeini, M. Ashkaboosi, P. Khazaei, and K. Mirzapalangi, "High performance control of grid connected cascaded H-bridge active rectifier based on type II-fuzzy logic controller with low frequency modulation technique," *International Journal of Electrical and Computer Engineering*, vol. 6, no. 2, pp. 484–494, Apr. 2016.
- [3] A. M. Bozorgi, V. Fereshtehpoor, M. Monfared, N. Namjoo, "Controller Design Using Ant Colony Algorithm for a Non-inverting Buck–Boost Chopper Based on a Detailed Average Model", *Electric Power Components and Systems*, vol. 43, no. 2. 2015.
- [4] A. M. Bozorgi, M. Monfared, and H. R. Mashhadi, "Optimum switching pattern of matrix converter space vector modulation," in *Computer and Knowledge Engineering (ICCKE)*, 2012 2nd International eConference on , 18-19 Oct. 2012 2012, pp. 89–93.
- [5] H. Jafarian, J. Enslin and B. Parkhideh "On Reactive Power Injection Control of Distributed Grid-tied AC-stacked PV Inverter Architecture" *Energy Conversion Congress and Exposition (ECCE)*, 2016, (In press)
- [6] M. Khodabandeh, M. R. Zolghadri and N. Noroozi, "A new t-type direct AC/AC converter," *The 6th Power Electronics, Drive Systems & Technologies Conference (PEDSTC2015)*, Tehran, 2015, pp. 247-252.
- [7] A. M. Bozorgi, M. Sanatkar Chayjani, R. Mohammad Nejad, and M. Monfared, "Improved grid voltage sensorless control strategy for railway power conditioners," *Power Electronics, IET*, vol. 8, pp. 2454-2461, 2015.
- [8] R. Rahimi, E. Afshari, B. Farhangi, and S. Farhangi, "Optimal placement of additional switch in the photovoltaic single-phase grid-connected transformerless full bridge inverter for reducing common mode leakage current," in *2015 IEEE Conference on Energy Conversion (CENCON)*, pp. 408-412, 2015.
- [9] M. Ashkaboosi, S. M. Nourani, P. Khazaei, M. Dabbaghjamanesh, and A. Moeini. "An optimization technique based on profit of investment and market clearing in wind power systems." *American Journal of Electrical and Electronic Engineering* 4, no. 3 (2016): 85-91.

- [10] S. Dusmez, M. Heydarzadeh, M. Nourani and B. Akin, "A robust remaining useful lifetime estimation method for discrete power MOSFETs," 2016 IEEE Energy Conversion Congress and Exposition, Milwaukee, WI, USA, 2016, pp. 1-6.
- [11] S. Ouni, M. Khodabandeh, M. Zolghadri, J. Rodriguez and H. Oraee, "A reduced switch cascaded transformer multi level inverter," 2015 IEEE 15th International Conference on Environment and Electrical Engineering (EEEIC), Rome, 2015, pp. 1013-1018.
- [12] Sahu, B., and Rincon-Mora, G.A. "A low voltage, dynamic, noninverting, synchronous buck-boost converter for portable applications," IEEE Trans on Power Electronics, Vol. 19, pp. 443-452, 2004.
- [13] Xiao, H., and Xie, S. "Interleaving double-switch buck-boost converter," IET Power Electronics, Vol. 5, pp. 899-908, 2012.
- [14] Schaltz, E., Rasmussen, P.O., and Khaligh, A. "Non-Inverting buck-boost converter for fuel cell applications," in: proceedings of 34th Annual IEEE Industrial Electronics IECON Conference, 2008.
- [15] STMicroelectronics, "An MCU-based low cost non-inverting buck-boost converter for battery chargers," Application. Rep. AN2389, STMicroelectronics, 2007.
- [16] Mohan, N., Undeland, T.M., and Robbins, W.P. "Power Electronics Converters, Applications, and Design," Third ed., Wiley, 2003.
- [17] A. M. Bozorgi, M. Monfared, and H. R. Mashhadi, "Two simple overmodulation algorithms for space modulated three-phase to three-phase matrix converter," IET Power Electron., vol. 7, no. 7, pp. 1915-1924, Jul. 2014
- [18] S. Jafarishiadeh, M. Ardebili, A. Nazari Marashi, "Investigation of pole and slot numbers in axial-flux pm bldc motors with single-layer windings for electric vehicles," 24th Iranian Conference on Electrical Engineering (ICEE), pp. 1444-1448, 2016.
- [19] S. M. Jafari-Shiadeh and M. Ardebili, "Analysis and comparison of axial-flux permanent-magnet brushless-DC machines with fractional-slot concentrated-windings", Proc. 4th Annu. Int. Power Electron., Drive Syst., Technol. Conf., pp. 72-77, 2013.
- [20] Khazaei, P., S. M. Modares, M. Dabbaghjamanesh, M. Almousa, and A. Moeini. "A high efficiency DC/DC boost converter for photovoltaic applications." International Journal of Soft Computing and Engineering (IJSCE) 6, no. 2 (2016): 2231-2307.
- [21] S. Jafari-Shiadeh, M. Ardebili, and P. Moamaei, "Three-dimensional finite-element-model investigation of axial-flux PM BLDC machines with similar pole and slot combination for electric vehicles", Proceedings of Power and Energy Conference, Illinois, pp. 1-4, 2015.
- [22] Z. Q. Zhu and D. Howe, "Improved Analytical Model for Predicting the Magnet Field Distribution in Brushless Permanent-Magnet Machines," IEEE Tran on Magn, vol. 38, pp. 229-238, 2002.

- [23] I. Mazhari, H. Jafarian, B. Parkhideh, S. Trivedi, and S. Bhowmik, "Locking Frequency Band Detection Method for Grid-tied PV Inverter Islanding Protection," IEEE Energy Conversion Congress and Exposition (ECCE), Montreal, QC, pp. 1976-1981, 2015.
- [24] P. Khazaei, M. Dabbaghjamanesh, A. Kalantarzadeh, and H. Mousavi. "Applying the modified TLBO algorithm to solve the unit commitment problem." In World Automation Congress (WAC), 2016, pp. 1-6. IEEE, 2016.
- [25] A. Bozorgi, M. Farasat, and S. Jafarishiadeh, "Improved model predictive current control of permanent magnet synchronous machines with fuzzy based duty cycle control," 2016 IEEE Energy Conversion Congress and Exposition (ECCE), Milwaukee, WI, USA, 2016, pp. 1-6.
- [26] Ferdowsi, Farzad, Ahmad Sadeghi Yazdankhah, and Bahareh Abbasi. "Declining power fluctuation velocity in large PV systems by optimal battery selection." In Environment and Electrical Engineering (EEEIC), 2012 11th International Conference on, pp. 983-988. IEEE, 2012.
- [27] Davoudi, A., and Jatskevich, J. "Realization of parasitics in state-space average-value modeling of PWM dc-dc converters," IEEE Trans on Power Electronics, Vol. 21, pp. 1142-1147, 2006.
- [28] Middlebrook, R.D., and Cuk, R. S. "A general unified approach to modeling switching converter power stages," IEEE PESC Record, 1976.
- [29] Lee, Y.J., Khaligh, A., and Emadi, A. "A compensation technique for smooth transitions in a noninverting buck-boost converter," IEEE Trans on Power Electronics, Vol. 24, pp. 1002-1015, 2009.
- [30] Safari, S., Ardehali, M. M., and Sirizi, M. J. "Particle swarm optimization based fuzzy logic controller for autonomous green power energy system with hydrogen storage," Energy Conversion and Management, Vol. 65, pp. 41-49, 2013.
- [31] Lefeuvre, E., Audigier, D., Richard, C., and Guyomar, D. "Buck-boost converter for sensorless power optimization of piezoelectric energy harvester," IEEE Trans on Power Electronics, Vol. 22, pp. 2018-2025, 2007.
- [32] Modabbernia, M., Kohani, F., Fouladi, R., and Nejati Sh. "The state-space average model of buck-boost switching regulator including all of the system uncertainties," International Journal on Computer Science and Engineering (IJCSSE), Vol. 5, pp. 120-132, 2013.
- [33] Ogata, K. Modern control engineering, fifth ed., Prentice Hall, 2010.
- [34] Erickson, R., and Maksimovic, D. Fundamental of power electronics, second ed., Springer, 2000.
- [35] Shiau, J.K., and Cheng, C.J. "Design of a non-inverting synchronous buck-boost DC/DC power converter with moderate power level," Robotics and Computer-Integrated Manufacturing, Vol. 26, pp. 263-267, 2010.
- [36] Kouchaki, A., Iman-eini, H., Asaei, B., "A new maximum power point tracking strategy for PV arrays

- under uniform and non-uniform insolation conditions," *Solar Energy*, Vol. 91, pp. 221-232, 2013.
- [37] M. Heydarzadeh and M. Nourani, "A Two-Stage Fault Detection and Isolation Platform for Industrial Systems Using Residual Evaluation," in *IEEE Transactions on Instrumentation and Measurement*, vol. 65, no. 10, pp. 2424-2432, Oct. 2016.
- [38] G. R. Moradi, E. Afshari, R. Rahimi, B. Farhangi and S. Farhangi, "Improvement of the modulation method for single-phase transformerless photovoltaic energy inverter for reactive power injection capability," 2016 24th Iranian Conference on Electrical Engineering (ICEE), Shiraz, 2016, pp. 1312-1317.
- [39] Ferdowsi, Farzad, Chris S. Edrington, and Touria El-mezyani. "Real-time stability assessment utilizing non-linear time series analysis." In *North American Power Symposium (NAPS)*, 2015, pp. 1-6. IEEE, 2015.
- [40] S. Dusmez; M. Heydarzadeh; M. Nourani; B. Akin, "Remaining Useful Lifetime Estimation for Power MOSFETs Under Thermal Stress With RANSAC Outlier Removal," in *IEEE Transactions on Industrial Informatics*, vol. PP, no. 99, pp. 1-1.
- [41] E. Afshari, R. Rahimi, B. Farhangi and S. Farhangi, "Analysis and modification of the single phase transformerless FB-DCB inverter modulation for injecting reactive power," 2015 IEEE Conference on Energy Conversion (CENCON), Johor Bahru, 2015, pp. 413-418.
- [42] Ferdowsi, Farzad, Ahmad Sadeghi Yazdankhah, and Homayoon Rohani. "A combinative method to control output power fluctuations of large grid-connected photovoltaic systems." In *Environment and Electrical Engineering (EEEIC)*, 2014 14th International Conference on, pp. 260-264. IEEE, 2014.
- [43] M. Khodabandeh, M. R. Zolghadri, M. Shahbazi and N. Noroozi, "T-type direct AC/AC converter structure," in *IET Power Electronics*, vol. 9, no. 7, pp. 1426-1436, 6 8 2016.